INTERNATIONAL JOURNAL FOR NUMERICAL METHODS IN FLUIDS
Int. J. Numer. Meth. Fluids **30**: 763–773 (1999)

LARGE EDDY SIMULATION IN A TURBULENT CHANNEL FLOW USING EXIT BOUNDARY CONDITIONS

T. CZIESLA, G. BISWAS[1] AND N.K. MITRA*

Institut für Thermo- und Fluiddynamik, Ruhr Universität Bochum, 44780 Bochum, Germany

SUMMARY

The influence of the exit boundary conditions on the vanishing first derivative of the velocity components and constant pressure on the large eddy simulation of the fully developed turbulent channel flow has been investigated for equidistant and stretched grids at the channel exit. Results show that the chosen exit boundary conditions introduce some small disturbances that are mostly damped by the grid stretching. The difference of rms values between the fully developed turbulent channel flow with periodicity conditions and the fully developed channel flow using inlet and the exit boundary conditions is less than 10% for the equidistant grids and less than 5% for the stretched grids. The chosen boundary conditions are of interest because they may be used in complex problems with back flow at the exit. Copyright © 1999 John Wiley & Sons, Ltd.

KEY WORDS: exit boundary conditions; turbulent flow; large eddy simulation

1. INTRODUCTION

Large eddy simulation of turbulent channel flows has been reported first by Kim and Moin [1] who considered a fully developed turbulent flow with periodicity conditions between the inlet and the exit of the computational domain. In such simulations, the problem of specification of the exit boundary condition can be avoided. The exit boundary condition for direct and large eddy simulation of turbulent flows plays a far more important role with respect to damping than for laminar flows. However, in real flows, the periodicity condition can be used more as an exception than as a rule. For example, in the case of impinging jet flows, periodicity conditions at the exit boundary can not be used.

Some investigations have been reported on the use of non-periodic exit conditions. Werner [2] has used vanishing first or second derivative conditions for the velocity components:

$$\frac{\partial^l U_i}{\partial X_1^l} = 0; \quad l = 1 \text{ or } 2. \tag{1}$$

* Correspondence to: Ruhr Universität Bochum, Institut für Thermo- und Fluiddynamik, Fakultat für Maschinenbau, 44780 Bochum, Germany.
[1] Current address: Department of Mechanical Engineering, Indian Institute of Technology, Kanpur-208016, India.

Contract/grant sponsor: Deutsche Forschungsgemeinschaft

CCC 0271–2091/99/140763–11$17.50

Received October 1997
Revised August 1998

Using such von Neumann-type boundary conditions he calculated turbulent channel flows via a Smagorinsky–Lilly [2] model. Such boundary conditions are often used for laminar flows, where only spatially smooth fields of flow variables exist. This means that further spatial development of flow is negligibly small.

Werner [2] pointed out that a very smooth field can be represented in Fourier space as one wave with a large wavelength together with far more waves with negligibly small wavelength. The difference form of the vanishing first derivative, corresponds exactly to waves with infinite wavelengths. The difference form of the vanishing second derivative with equidistant grids corresponds to a wave of infinite length and a wave with finite length, which is large related to the grid distances.

In contrast to laminar flows one can find very large gradients in turbulent flows, i.e. very rough fields. So there are also waves with short wavelengths (high frequencies) that are reflected at the exit boundary. These reflections mean disturbances to the results of the computational domain. Finally, it should be mentioned that vanishing higher derivatives as exit conditions can lead to numerical instabilities [2].

An alternative class of boundary conditions are the so-called 'non-reflecting boundary conditions', which were originally developed for hyperbolic equations [3–6,17].

Jin and Braza [7] used such a condition for an elliptic problem. They calculated the transition of free shear layers using the two-dimensional incompressible unsteady Navier–Stokes equations.

The basic idea of their boundary condition formulation is the requirement that the waves of short length could pass through the boundary without being reflected. Based on the two-dimensional wave equation

$$\frac{\partial^2 u_i}{\partial t^2} - c_x^2 \frac{\partial^2 u_i}{\partial x^2} - c_y^2 \frac{\partial^2 u_i}{\partial y^2} = 0, \tag{2}$$

they developed the following

$$\frac{\partial u_i}{\partial t} + u_1 \frac{\partial u_i}{\partial x} - \nu \frac{\partial^2 u_i}{\partial y^2} = 0, \tag{3}$$

where u_1 is the velocity in the main flow direction.

Comparison of the coefficients of this equation with the Navier–Stokes equation provides the matched form of the equation [3].

Another formulation of non-reflecting boundary condition is presented by Bestek *et al.* [8] for calculation of transition of boundary layers, based on the velocity–vorticity formulation of the Navier–Stokes equations. The second derivatives, in the main flow direction (normal to the exit plane) are set to zero. So there is a damping that leads to a relaminarization of the flow near to the exit plane and the reflection of disturbances is decreased.

Richter *et al.* [9,10] have used 'frozen turbulence' as the boundary condition in flow with pressure gradient. This technique is based on the assumption that the time variation of the turbulent fluctuations (the difference of instantaneous values of the flow variables from their average values) depends on the convective transport, i.e. the instantaneous values at the exit plane depend on the ones directly at the upstream. Richter *et al.* [9,10] developed a relationship between the fluctuations at the exit plane and the plane directly upstream of the exit,

$$\Phi''(n_x, j, k)\big|_n = \Phi''(il, j, k)\big|_{n-\Delta n}, \tag{4}$$

$$\Delta n(j, k) = \frac{\Delta x}{[\Delta t \cdot u_c(j, k)]} \tag{5}$$

where u_c is the characteristic convective velocity at the exit in the x-direction and is set equal to $\langle u(il, j, k)\rangle$. The sign, $\langle\ \rangle$ symbolizes the time-averaged value. It is necessary to save enough time levels (Δn levels for getting $\Phi''|_{n-\Delta n}$) for implementation of this boundary condition. With the following equation

$$\Phi(i, j, k) = \tilde{\Phi}(i, j, k) + \Phi''(i, j, k), \tag{6}$$

the values at the exit plane can be defined. The average value Φ is calculated by using a linear extrapolation of the variables from the interior points.

The purpose of the present work is to perform a LES for fully developed turbulent flows in a rectangular channel with an exit boundary condition and compare the results with computations with periodicity conditions in order to determine the influence of the boundary condition (see Figure 1). The underlying idea is to use an exit boundary condition on a channel with fully developed turbulent flow at the entry. It is expected that the flow will remain fully developed turbulent and the chosen exit boundary condition should have a negligible effect on the flow.

For velocity boundary conditions it was decided to use the vanishing first derivative conditions like Werner [2] described above. One important aspect for this choice was the experience [11] that this condition in principle allows the calculation of complex flow structures like backflow at the exit plane caused by the entrainment. So it is interesting to investigate such a condition because there are no exact formulations for the LES for such flows (like jets, impinging jets, etc.) so far. The flow field of interest is non-periodic and a backflow may appear at the exit. Jin and Braza [7] showed good results for the simulation of the two-dimensional Navies–Stokes equations for transitional free shear flow. But it is not known if their non-reflecting conditions are suitable for calculating three-dimensional turbulent flows by LES too. Besides, their boundary condition will not allow backflow at the exit plane. Same is true for the condition used by Bestek *et al.* [8]. The 'frozen turbulence' condition from Richter *et al.* [9] is expensive because of the necessity of large computer time for sampling the variables at different time levels.

2. NUMERICAL METHOD

Consider a rectangular channel of length L (see Figure 1). A periodicity boundary condition at $x = 0$ and $x = L/2$ is used so that fully developed turbulent flow is simulated. Then the computation is further continued to $x = L$, where an exit boundary condition is used. A comparison of the flow fields at the first and the second channel (Figure 1) would show the influence of the exit boundary conditions. The filtered (top hat filter is used) continuity and Navier–Stokes equations are

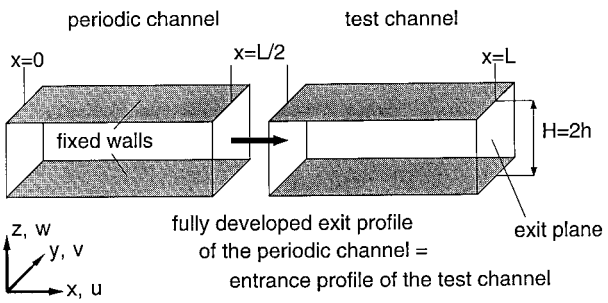

Figure 1. Schematic of the geometry.

$$\frac{\partial \bar{u}_i}{\partial x_i} = 0,$$
$$\frac{\partial \bar{u}_i}{\partial t} = -\frac{\partial \bar{p}}{\partial x_i} - \frac{\partial \bar{u}_i \bar{u}_j}{\partial x_j} - \frac{\partial \overline{u'_i u'_j}}{\partial x_j} + \frac{1}{Re_\tau}\frac{\partial^2 \bar{u}_i}{\partial x_j^2}. \tag{7}$$

For the subgrid scales, the Smagorinsky–Lilly model is used (with $C_s = 0.1$).

$$\tau_{ij} = \overline{u'_i u'_j} = -2\nu_T \bar{S}_{ij} + \frac{\delta_{ij}}{3}\overline{u'_k u'_k}, \tag{8}$$

$$\nu_T = (C_s \cdot \Delta)^2 (2\bar{S}_{ij}\bar{S}_{ij})^{1/2} \tag{9}$$

and

$$\bar{S}_{ij} = \frac{1}{2}\left(\frac{\partial \bar{u}_i}{\partial x_j} + \frac{\partial \bar{u}_j}{\partial x_i}\right). \tag{10}$$

3. BOUNDARY CONDITIONS

No-slip conditions have been used on the walls for the convective terms. The no-slip condition for the diffusive terms were implemented by using the Schumann assumption [12] in conjunction with the logarithmic law of the wall. Periodicity conditions have been used at $x = 0$ and $x = L/2$. At $x = L$ we use

$$\frac{\partial u_i}{\partial x_1} = 0$$

and

$$p = \text{constant}.$$

Use of the coupled vanishing first derivative boundary condition with $p = \text{constant}$ is based on an outflow boundary condition of Rannacher [13]. Earlier investigations showed that these conditions are suitable for the calculation of backflow caused by entrainment. The assumption of constant pressure is acceptable because at the exit plane, the fluid leaves the computational domain towards the ambience with a constant pressure.

The handling of backflow is obviously one of the biggest problems for simulation of impinging jet flow (see Hoffmann and Benocci [14]). Some authors presented conditions where the assumption of vanishing first derivatives in main flow direction for the base flow [15] is necessary. But this enlarges the computational domain and thereby the computational time. Because the authors want to investigate impinging jet flows by LES in future, they decided to select the conditions mentioned above.

4. METHOD OF SOLUTION

The basic equations have been solved by a fractional step method of Kim and Moin [1], which uses Adams–Bashforth and Crank–Nicholson difference schemes and a SIP solver (Stone [16]) for the numerical solution of the pressure Poisson equation.

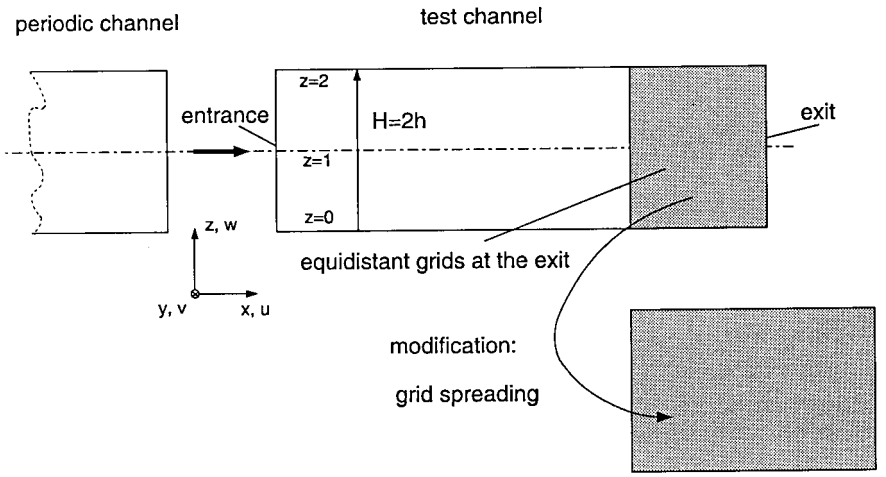

Figure 2. Schematic of the computational scheme.

5. RESULTS AND DISCUSSION

The Reynolds number based on the friction velocity and half of the channel height is

$$Re_\tau = \frac{u_\tau(h/2)}{\nu} = 180.$$

Each channel was discretized using $34 \times 34 \times 18 = 20808$ grids. The non-dimensional length in the x-direction was 8.5 for each half, in the y-direction 4 and in the z-direction 2 ($\Delta x = 0.25$, $\Delta y = \Delta z = 0.125$).

Besides, another modification was included during the implementation of the exit boundary condition.

The length of the second half of the channel, i.e. the part where it was intended to investigate the influence of the boundary condition, is increased to $L = 9.145$ by stretching the last eight grid cells in the x-direction steadily by 10% of the grid distance of the upsteam neighbouring cell (see Figure 2). With this stretching, the numerical viscosity is increased. This stretching is probably equivalent to a buffer layer. The computations reveal how the non-equidistant grids influence the results *vis a vis* the case of equidistant grids.

For the investigation of the influence of the boundary conditions, the second channel is divided in two parts (each part with 17 grid cells, see Figure 2) so that one can observe the influence of the exit plane in the upstream direction.

Figures 3–5 compare the distribution of the different rms values in the three dimensions. Obviously, the rms values for the channel with the experimental boundary conditions are higher than that of the periodic channel. The plots for the two parts of the channel with these boundary conditions are nearly identical. This indicates an influence of the exit boundary condition through the whole channel. The rms values for the test cases show nearly constant deviation from the values of periodic channel near the core.

In Table I, the local maxima (max) and minima (min) of each rms component of the periodic and the two parts of the test channel are compared. The differences of the each part of the second channel expressed in percent are related to the periodic channel. The values of the two parts of the test channel differs at both maxima and minima. But the largest difference,

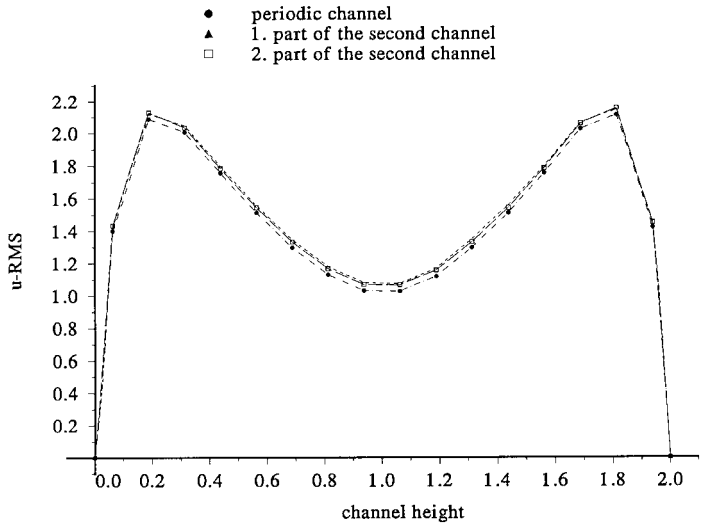

Figure 3. *u* rms, equidistant grid.

the rms value in the *y*-direction, is only 10.27%. All of the other differences are lower. This boundary condition introduces a disturbance in the whole test channel, which is expressed by higher rms values. But the effect of this disturbance is relatively low. Both parts of the test channel are influenced equally.

It may be mentioned that the differences of the maximum rms values are smaller than the differences of the minimum values (see Table I). This means that the locations where the fluctuation level is high are less influenced than the locations where the fluctuation level is low.

Figures 6–8 show the distribution of rms values of velocity components for the case of grid spreading. The profiles are qualitatively similar to those obtained by Kim *et al.* [18] who validated their results against experiments. The values of the first part of the test channel are

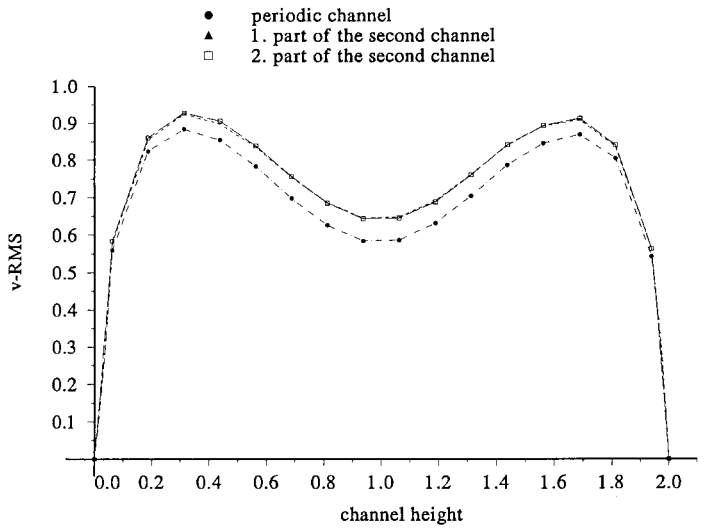

Figure 4. *v* rms, equidistant grid.

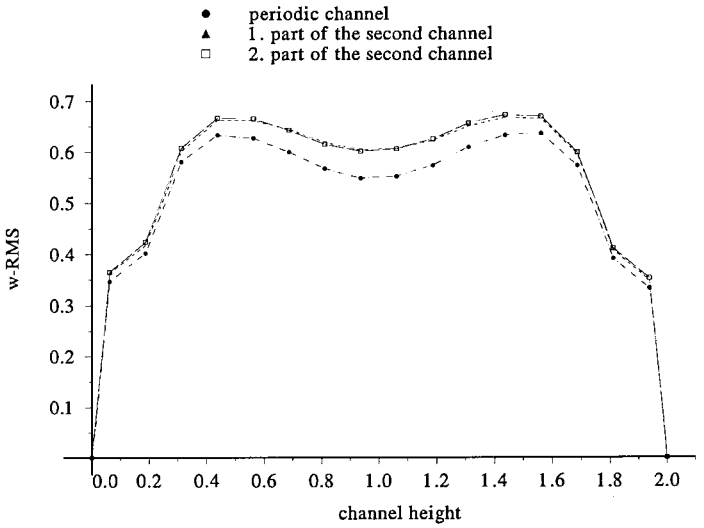

Figure 5. *w* rms, equidistant grid.

above the values of the periodic channel. The values of the second part are equal or, slightly lower than the values of the periodic channel. This indicates a decrease in the fluctuations because of the damping effect of the grid spreading. Table II shows the maximum and minimum rms values and the differences of the two parts of the test channel from the periodic channel. The mentioned tendencies can be confirmed again. The rms values of the first part are higher than that of the periodic channel, but lower than that due to the equidistant grids (see Table I). All of the values of the second part are even lower than the values of the periodic channel. This means, that in the case of grid spreading, there is also an influence of the boundary condition. But as compared with the case of equidistant grid a decrease in the differences with regard to the periodic channel could be achieved. The reason is the increase of the damping effect via numerical viscosity because of the grid spreading. This spreading influences very strongly the calculation of the rms values of the second half of the test channel. In this part the damping effect is larger. This explains the cause of low rms values.

Table I. Comparison of local maxima (Max) and minima (Min) for different 1D ensemble-averaged values, *equidistant grid*[a]

		Periodic channel	1. Part test channel	2. Part test channel	Difference of 1 (%)	Difference of 2 (%)
u rms	Min	1.028	1.075	1.067	4.85	3.88
	Max	2.112	2.146	2.154	1.61	1.99
v rms	Min	0.584	0.644	0.643	10.27	10.10
	Max	0.883	0.924	0.928	4.64	5.10
w rms	Min	0.549	0.604	0.601	10.02	9.47
	Max	0.635	0.666	0.672	4.88	5.83
Reynolds stress	Min	−0.519	−0.543	−0.551	−4.62	−6.17
	Max	0.529	0.554	0.550	4.73	3.97

[a] Averaging was done in the *x*- and *y*-direction; the differences of each part of the second (test-) channel expressed in percent are referred to the values of the periodic channel.

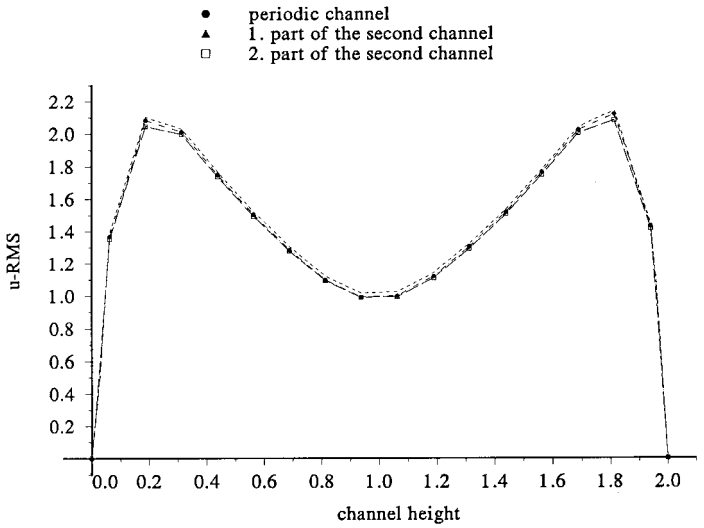

Figure 6. *u* rms, non-equidistant grid.

Figures 9 and 10 show the Reynolds stresses on the *xz*-plane. Results are comparable with those of Reference[18]. Table I compares the maximum and minimum values of the Reynolds stresses. One can point out that the simulation using the present boundary condition yields acceptable results. In the case of equidistant grids, the maximum difference from the periodic case for the local maxima and minima is -6.17% (see Table I, the negative sign results from the definition of the axis system). The comparison of the averaged centerline velocity confirm this conclusion (see Tables III and IV).

In the case of grid spreading, the results are even better, see Figure 10 and Table IV. Here the maximum difference for the comparison of the local maxima and minima is only 2.4%. The comparison of the centerline velocities shows correct trend.

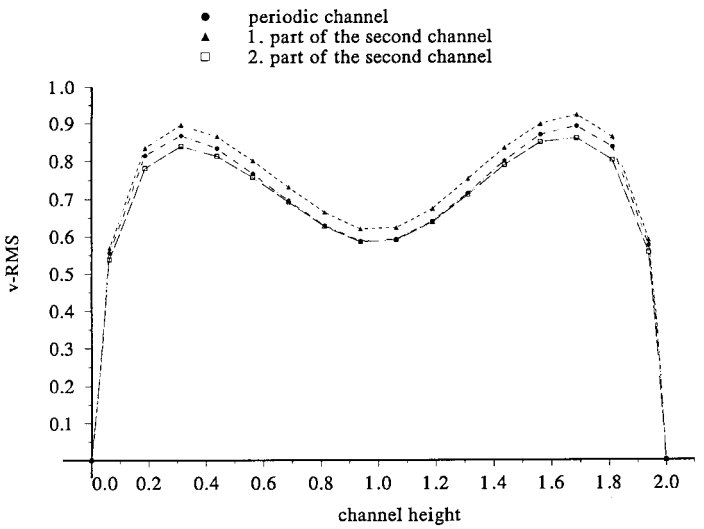

Figure 7. *v* rms, non-equidistant grid.

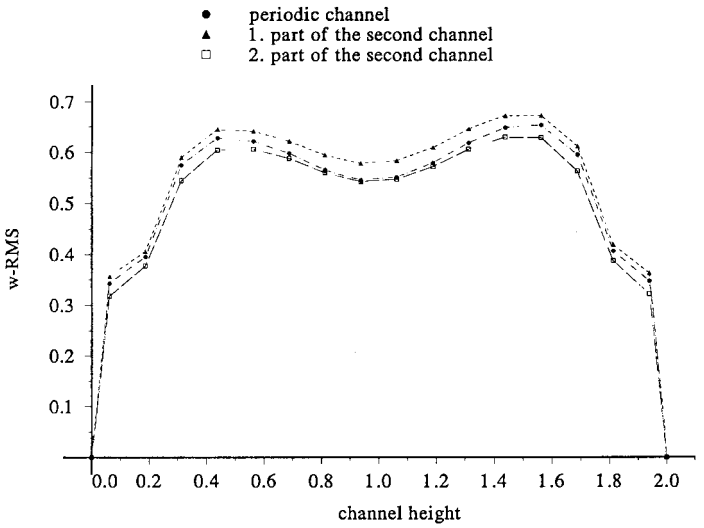

Figure 8. w rms, non-equidistant grid.

6. CONCLUSION

The influence of the coupled exit boundary conditions of Neumann and Dirichlet type on LES of turbulent channel flows has been investigated. A comparison of the results with the that of a channel using periodic boundary condition has been made. Besides, a modification based on grid stretching near the exit plane in conjunction with the proposed boundary conditions has been presented.

The results confirm the conjecture, that the disturbance caused by the boundary conditions at the exit plane is transported in the upstream direction. The influence of the chosen boundary conditions lead to slightly increased turbulent fluctuations. This behaviour is expressed by higher rms values.

The results with grid spreading, because of the increased damping of non-equidistant grids, show better agreement with the fully developed results.

Table II. Comparison of local maxima (Max) and minima (Min) for different 1D esemble-averaged values, *non-equidistant grid*[a]

		Periodic channel	1. Part test channel	2. Part test channel	Difference of 1 (%)	Difference of 2 (%)
u rms	Min	0.992	1.016	0.989	2.42	−0.30
	Max	2.117	2.139	2.081	1.04	−1.70
v rms	Min	0.587	0.620	0.584	5.62	−0.51
	Max	0.891	0.921	0.859	3.37	−3.59
w rms	Min	0.545	0.578	0.542	6.06	−0.55
	Max	0.653	0.671	0.629	2.76	−3.68
Reynolds stress	Min	−0.535	−0.540	−0.526	−0.93	1.68
	Max	0.513	0.518	0.501	0.97	−2.40

[a] Averaging was done in the x- and y-direction; the differences of each part of the second (test-) channel expressed in percent are referred to the values of the periodic channel.

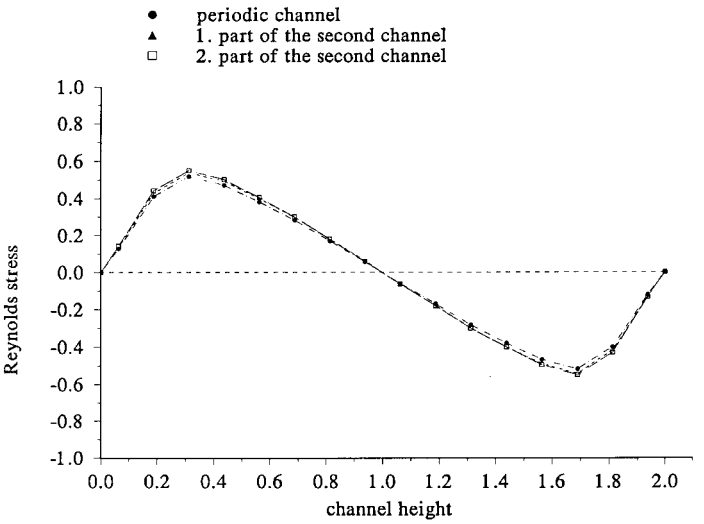

Figure 9. Reynolds stresses (*uw* component in *xz*-plane).

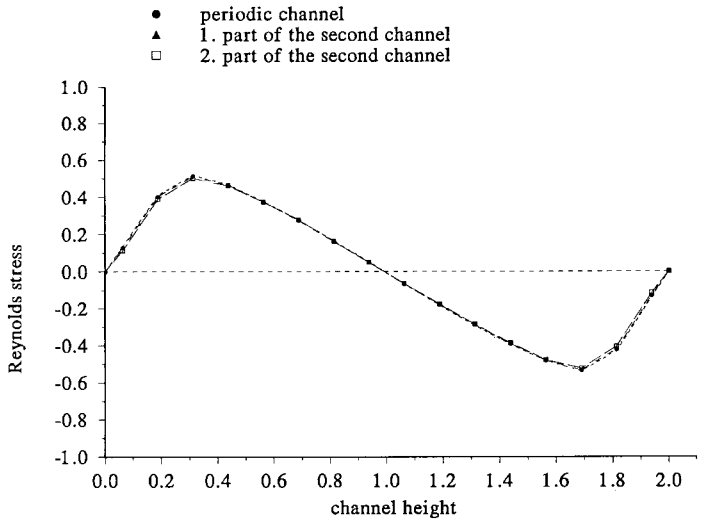

Figure 10. Reynolds stresses (*uw* component in *xz*-plane).

Table III. Comparison of the averaged centerline velocities, *equidistant grid*

	Periodic channel	1. Part test channel	2. Part test channel	Difference of 1 (%)	Difference of 2 (%)
Centerline velocity	18.65	18.57	18.54	−0.43%	−0.59%

Table IV. Comparison of the averaged centerline velocities, *non-equidistant grid*

	Periodic channel	1. Part test channel	2. Part test channel	Difference of 1 (%)	Difference of 2 (%)
Centerline velocity	18.58	18.51	18.48	−0.38%	−0.53%

It was also found that the disturbance caused by the boundary conditions is small at places where the flow fluctuates strongly. One can expect that this boundary condition will yield good results for other complex flows especially with high turbulent fluctuations.

ACKNOWLEDGMENTS

The authors thank the Deutsche Forschungsgemeinschaft for financial support of this project.

REFERENCES

1. J. Kim and P. Moin, 'Application of a fractional step method to incompressible Navier-Stokes equations', *J. Comput. Phys.*, **59**, 308–323 (1985).
2. H. Werner, 'Grobstraktursimulation der turbulenten Strömung über eine querliegende Rippe in einem Plattenkanal bei hoher Reynoldszahl', Dissertation Universität München, 1991.
3. B. Enquist and A. Majda, 'Numerical radiation boundary conditions for unsteady transonic flow', *J. Comput. Phys.*, **40**, 91–103 (1981).
4. B. Gustaffson and H.O. Kreiss, 'Boundary conditions for time dependent problems with an artificial boundary', *J. Comput. Phys.*, **30**, 333–351 (1979).
5. T.Y. Han, J.C.S. Meng and G.E. Innis, 'An open boundary condition for incompressible stratified flows', *J. Comput. Phys.*, **49**, 276–297 (1983).
6. G.W. Hedstrom, 'Non-reflecting boundary conditions for non-linear hyperbolic systems', *J. Comput. Phys.*, **30**, 222–237 (1979).
7. G. Jin and M. Braza, 'A non-reflecting outlet boundary condition for incompressible unsteady Navier–Stokes calculations', *J. Comput. Phys.*, **107**, 239–253 (1993).
8. H. Bestek, M. Kloker and W. Müller, 'Spatial direct numerical simulation of boundary layer transition under strong adverse pressure gradient', *Proc. 74th AGARD Fluid Dynamics Panel Symposium 'Application of Direct and Large Eddy Simulation to Transition and Turbulence'*, Chania, Greece, April 18–21, 1994.
9. K. Richter, 'Grobstruitursimulation Turbulenter Wandscherschichten mit Wärmetransport', Dissertation Technische Universität München, 1988.
10. K. Richter, R. Friedrich and L. Schmitt, 'Large eddy simulation of turbulent wall boundary layers with pressure gradient', *Sixth Symposium on 'Turbulent Shear Flows'*, Toulouse, France, September 7–9, 1987.
11. H. Laschefski, 'Numerische Untersuchung der dreidimensionalen Strömungsstraktur und des Wärmeübergangs bei ungeführten und geführten Freistrahlen mit Prallplatte', Dissertation Ruhr-Universität Bochum, 1993.
12. U. Schumann, 'Subgrid-scale model for finite difference simulations of turbulent flows in plane channels and annuli', *J. Comput. Phys.*, **18**, 376–404 (1975).
13. R. Rannacher, 'On the numerical solution of the incompressible Navier–Stokes equations', *Preprint 92-12* Universität Heidelberg, Vortrag auf der GAMM-Jahrestagung in Leipzig, 24–27.3, 1992.
14. G. Benocci and C. Hoffmann, 'Numerical simulation of spatially-developing planar jets', *Proc. AGARD Fluid Dynamic Panel Symposium*, Chania, Greece, April 18–21, 1994.
15. J. Nordström, 'Accurate solutions of the Navier–Stokes equations despite unknown boundary data', *J. Comput. Phys.*, **120**, 184–205 (1995).
16. H.L. Stone, 'Iterative solution of implicit approximations of multidimensional partial differential equations', *SIAM J. Numer. Anal.*, **5**, 530–558 (1968).
17. I. Orlanski, 'A simple boundary condition for unbounded hyperbolic flows', *J. Comput. Phys.*, **21**, 251–269 (1976).
18. J. Kim, P. Moin and R. Moser, 'Turbulence statistics in fully developed channel flow at low Reynolds number', *J. Fluid Mech.*, **177**, 133–166 (1987).

